JOURNAL OF GEOPHYSICAL RESEARCH, VOL. 106, NO. A11, PAGES 26,137–26,146, NOVEMBER 1, 2001

Morphology and time variability of Io's visible aurora

P. E. Geissler,[1] W. H. Smyth,[2] A. S. McEwen,[1] W. Ip,[3] M. J. S. Belton,[4] T. V. Johnson,[5] A. P. Ingersoll,[6] K. Rages,[7] W. Hubbard,[1] and A. J. Dessler[1]

Abstract. Clear-filter imaging of Io during the Galileo nominal and extended missions recorded diffuse auroral emissions in 16 distinct observations taken during 14 separate eclipses over a two year period. These images show that the morphology and time variability of the visible aurora have several similarities to Io's far ultraviolet emissions. The orbital leading hemisphere of Io is consistently brighter than the trailing hemisphere, probably due to a greater concentration of torus electrons in the wake region of the satellite. The locations of the polar limb glow and the bright equatorial glows appear to correlate with Io's System III longitude. Unlike the far ultraviolet emissions, the visible aurorae are enhanced near actively venting volcanic plumes, probably because of molecular emission by SO_2.

1. Introduction

Visible emissions from Io during eclipse by Jupiter were first detected by the Voyager 1 spacecraft [*Cook et al.*, 1981]. Detailed images of these optical aurorae have now been acquired by both Galileo, in orbit around Jupiter since 1996, and Cassini as it sped through the Jovian system in early 2001 en route to Saturn. The highest-resolution images were recorded by the Galileo Solid State Imaging (SSI) system [*Belton et al.*, 1996]. Some aspects of the auroral morphology, colors and time variability were described from SSI color observations by *Geissler et al.* [1999]. Three distinct emissions were noted in color images taken during orbit 15 with SSI's violet (380-445 nm), green (510-605 nm), red (615-710 nm), and clear (380-1040 nm) filters. Bright blue glows occur along the equator near the sub-Jupiter and anti-Jupiter points (longitudes 0 and 180), apparently associated with active volcanic plumes; a red glow appears along the limb, brightest near the pole that is closest to the plasma torus center; and a faint emission distributed across the disk of Io was seen in the SSI green-filter images. Ground-based [*Bouchez et al.*, 2000; *Oliversen et al.*, this issue] and Hubble Space Telescope (HST) [*Trauger et al.*, 1997; *Retherford et al.*, 1999; *Oliversen et al.*, 2000] observations suggest neutral atomic oxygen ([OI] 630 and 636 nm) to be the likely emitter of the red glows, whereas neutral sodium D lines (589 and 590 nm) probably account for the green-filter emissions. No atomic lines have been identified in the wavelength interval from 380 to 445 nm to explain the intense blue equatorial glows, and it is believed that they are caused instead by electron excitation of molecular SO_2 [cf. *Miller and Becker*, 1987; *Ajello et al.*, 1992]. The Galileo orbit 15 data indicated some temporal variability of the emissions in the form of a ~30% reduction in the disk-averaged brightness of Io in a pair of clear-filter images taken over a 42 minute interval as the satellite remained in Jupiter's shadow [*Geissler et al.*, 1999]. Curiously, the equatorial glows did not dim during this interval but instead brightened by a comparable amount.

Visible emissions from neutral atomic oxygen ([OI] 630 and 636 nm) have been studied for more than a decade using telescopic observations [*Scherb and Smyth*, 1993; *Scherb et al.*, 1999; *Oliversen et al.*, this issue], augmented by images from HST Wide Field and Planetary Camera (WFPC2) [*Trauger et al.*, 1997] and Space Telescope Imaging Spectrograph (STIS) [*Retherford et al.*, 1999; *Oliversen et al.*, 2000]. The HST images, taken with Io in eclipse by Jupiter, show enhanced emission on the wake side of Io (the orbital leading hemisphere, centered at longitude 90), along with polar limb glows that vary with Io's magnetic latitude, appearing brighter on the pole of Io that faces the magnetic equator. Bright glows also appear near the sub-Jove point (the anti-Jove point can not be seen in these observations). The extensive temporal and longitudinal coverage of the telescopic observations has shown that the emissions are correlated with the moon's magnetic longitude (the location of Io in Jupiter's magnetic field) but also vary markedly in intensity over time periods at least as short as the 20 minute resolution of the observations.

Ultraviolet emissions from neutral atomic oxygen and sulfur are also highly variable, as demonstrated by IUE mission measurements and the Goddard High-Resolution Spectrograph (GHRS) and Faint Object Spectrograph (FOS) instruments on HST [*Ballester et al.*, 1987, 1996, 1997; *Clarke et al.*, 1994]. Recent STIS images [*Roesler et al.*, 1999; *Retherford et al.*, 2000] of Io's OI 135.6 nm and SI 190.0 nm emissions show details of the ultraviolet emission morphology that are similar to the visible glows. Equatorial bright spots occur near the sub-Jove and anti-Jove points that move about with the changing orientation of Jupiter's magnetic field and appear uncorrelated with the locations of volcanic vents. The outer glow on the anti-Jovian side of Io tends to be brighter than the inner equatorial glow, perhaps due to rotation of Io's electric field by the Hall effect [*Saur et al.*, 2000] or

[1]Lunar and Planetary Laboratory, University of Arizona, Tucson, Arizona, USA
[2]Atmospheric and Environmental Research, Inc., Cambridge, Massachusetts, USA.
[3]Institute of Astronomy, National Central University, Chung-Li, Taiwan, ROC.
[4]Belton Space Exploration Initiatives, Tucson, Arizona, USA
[5]Jet Propulsion Laboratory, California Institute of Technology,Pasadena, California, USA
[6]Division of Geology and Planetary Sciences, California Institute of Technology, Pasadena, California, USA.
[7]Space Physics Research Institute, Sunnyvale, California, USA

Paper number 2000JA002511.
0148-0227/01/2000JA002511$09.00

Table 1. Nominal and Extended Mission Clear-Filter Eclipse Images

Image Number	Plate 1 Letter	Orbit and Picture Number	Date	Greenwich Mean Time	Exposure Time, s	Center Latitude and Longitude, deg		Resolution, km pixel^{-1}	λ_{III}, deg	Elapsed Time in Eclipse, min
350029700	h	G1I0030	June 29, 1996	03:46:18	2.1	2.76	234.78	10.49	189	46.5
374478046	k	E4I0002	Dec. 17, 1996	19:46:10	8.5	-0.20	36.17	17.63	218	32.9
383809200	a	E6I0070	Feb. 21, 1997	08:14:22	6.4	0.45	295.79	9.19	4	79.1
389608268	i	G7I0001	April 3, 1997	01:29:25	6.4	-0.27	60.68	33.29	165	94.2
394394200	l	G8I0003	May 6, 1997	16:00:26	6.4	-0.80	75.43	18.56	261	60.5
401957745	c	C9I0026	June 28, 1997	18:36:17	6.4	0.12	280.41	14.60	47	77.5
413546765	n	10I0001	Sept. 18, 1997	03:34:03	6.4	-0.22	46.84	13.27	326	19.6
413799045	d	10I0046	Sept. 19, 1997	22:04:53	6.4	0.26	275.95	11.44	68	22.9
416072400	m	10I0100	Oct. 5, 1997	21:11:02	6.4	0.18	180.76	62.82	276	71.8
420361500	j	11I0003	Nov. 4, 1997	23:58:31	6.4	-0.38	104.32	17.96	205	113.2
420858600	b	11I0027	Nov. 8, 1997	11:44:45	6.4	0.20	256.25	13.76	13	42.2
441026800	e	14I0019	March 30, 1998	02:27:30	6.4	0.28	296.24	11.51	156	68.3
449843800	o	15I0004	May 31, 1998	00:17:07	6.4	-0.33	68.23	13.97	53	10.8
449847913	p	15I0022	May 31, 1998	00:58:43	6.4	-0.34	72.20	13.42	72	52.4
450096313	f	15I0043	June 1, 1998	18:50:19	6.4	0.12	298.22	10.91	156	14.2
450101513	g	15I0053	June 1, 1998	19:42:54	6.4	0.13	301.85	11.50	180	66.7

asymmetries in the flux of impacting electrons [e.g., *Peratt and Dessler*, 1988]. Polar limb glows are observed that are brightest on the hemisphere facing the magnetic equator. Extended UV emissions also occur in the wake of Io [*Ballester et al.*, 1997; *Wolven et al.*, 1999, this issue].

Eclipse imaging of Io was undertaken periodically throughout the Galileo mission, in part to monitor thermal emission from Io's many active volcanoes [*McEwen et al.*, 1998a, 1998b]. The multispectral images discussed by *Geissler et al.* [1999] were limited to the leading hemisphere of Io and showed only snapshots of the aurorae at specific times. In order to investigate the global morphology of Io's visible emissions, their time variability, and their relationship to the ultraviolet emissions we undertook a study of the complete set of Galileo clear-filter eclipse images. Because of their broad band pass, the clear-filter images record a variety of phenomena including both atomic and molecular emissions. We find many similarities between the visible and ultraviolet aurorae, suggesting that they are excited by a common population of electrons. We also note important differences that are likely due to local concentrations of gas derived from active volcanic vents.

2. Observations

2.1 Emission Morphology

Table 1 lists the images considered for this study. These include all clear-filter eclipse images acquired during the Galileo nominal and extended missions that were adequately exposed to show diffuse atmospheric emissions. They include 16 images acquired during 14 separate eclipses on 10 spacecraft orbits over the course of 2 years. Plate 1 shows these images ordered by Io's System III Jovian magnetic longitude (λ_{III}) and divided into wake-side (orbital leading hemisphere) and nonwake (trailing hemisphere) views. Two of the images (Plates 1b and 1d) are contaminated by moonlight reflected from Europa. Two others (Plates 1f and 1o) were recorded within 15 minutes of eclipse ingress and may be affected by Jupiter shine (sunlight scattered into Jupiter's shadow by aerosols in Jupiter's upper atmosphere).

Bright equatorial glows are visible near the sub-Jupiter and anti-Jupiter points in all of these pictures. Their shapes vary widely with time, ranging from thin limb glows through umbrella-shaped plumes to extended emissions rising as much as 700 km from the surface. In general, the locations of these equatorial glows correspond to the tangent points of the Jovian magnetic field lines (indicated by dots in the adjacent diagrams). This oscillation in latitude is particularly apparent in Plates 1a and 1e, two pictures taken with nearly the same viewpoint (subspacecraft longitude) but widely separated in time. The few exceptions to the correspondence between equatorial glow location and Jovian magnetic field orientation appear to be areas of enhanced emission associated with specific volcanic centers, such as Acala (11°N, 335°W) on the right side of Plate 1i and Acala and Prometheus (2°S, 153°W) in Plate 1l. Even so, a bright zone can be seen along the limb to the south of Acala in Plate 1i, in the neighborhood of the magnetic field line tangent point. Moreover, local brightening along the limb can be seen near the tangent points even when no volcanic vents appear to be active, for example in Plate 1a. Another correlation with System III longitude can be seen in the emissions near the poles of Io. The limb glow is enhanced for the polar hemisphere closest to the equator of the Jovian magnetic field (indicated by a horizontal line in the adjacent diagrams). In addition, faint emissions can be seen across the disk of Io, conspicuous in the wake-side views but largely absent from the tailing hemisphere.

The relationship between equatorial glows and volcanic vents is more clearly seen in Figure 1. Figure 1 compares the eclipse images to diagrams charting the locations of volcanic vents known to be active during the Galileo mission [*McEwen et al.*, 1998a, Table VI]. Vents located on the side of Io viewed in each image are shown as white dots, while those on the opposite side of Io are shown in black (only those black dots near the limb contributed to the emissions visible in each image). Most of the vents were active episodically; only Prometheus (2°S, 153°W) was clearly active in every image with the appropriate geometry, although several other fainter plumes may have been continuously active as well. Two characteristics of Io's equatorial glows are evident from inspection

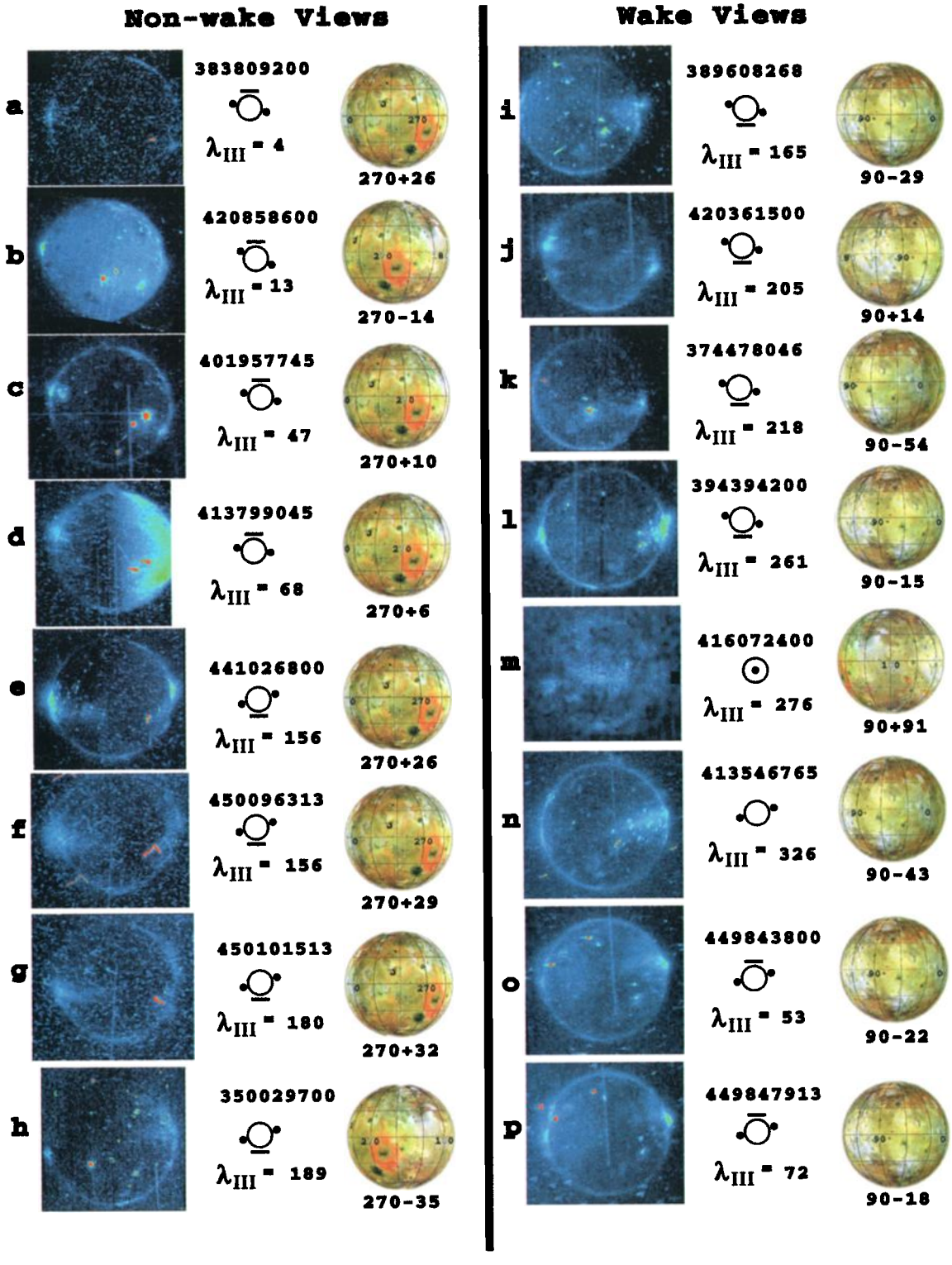

Plate 1. (a-p) Calibrated Galileo clear-filter eclipse images. Ordered by Io System III longitude, the 16 Galileo clear-filter eclipse images of Io considered for this study are shown divided into views of the orbital leading hemisphere (wake views) and trailing hemisphere (nonwake). They are color-coded so that blue represents emissions from 0 to 7.5 nW cm^{-2} sr^{-1}, green shows emissions from 7.5 to 15 nW cm^{-2} sr^{-1}, and red shows emissions >15 nW cm^{-2} sr^{-1} (just the volcanic hot spots and field stars are red). Corresponding maps of the satellite are shown for reference. Also shown are cartoons crudely illustrating the locations of the tangent points of Jovian magnetic field lines during each observation (dots) and the direction of the plasma torus center (line).

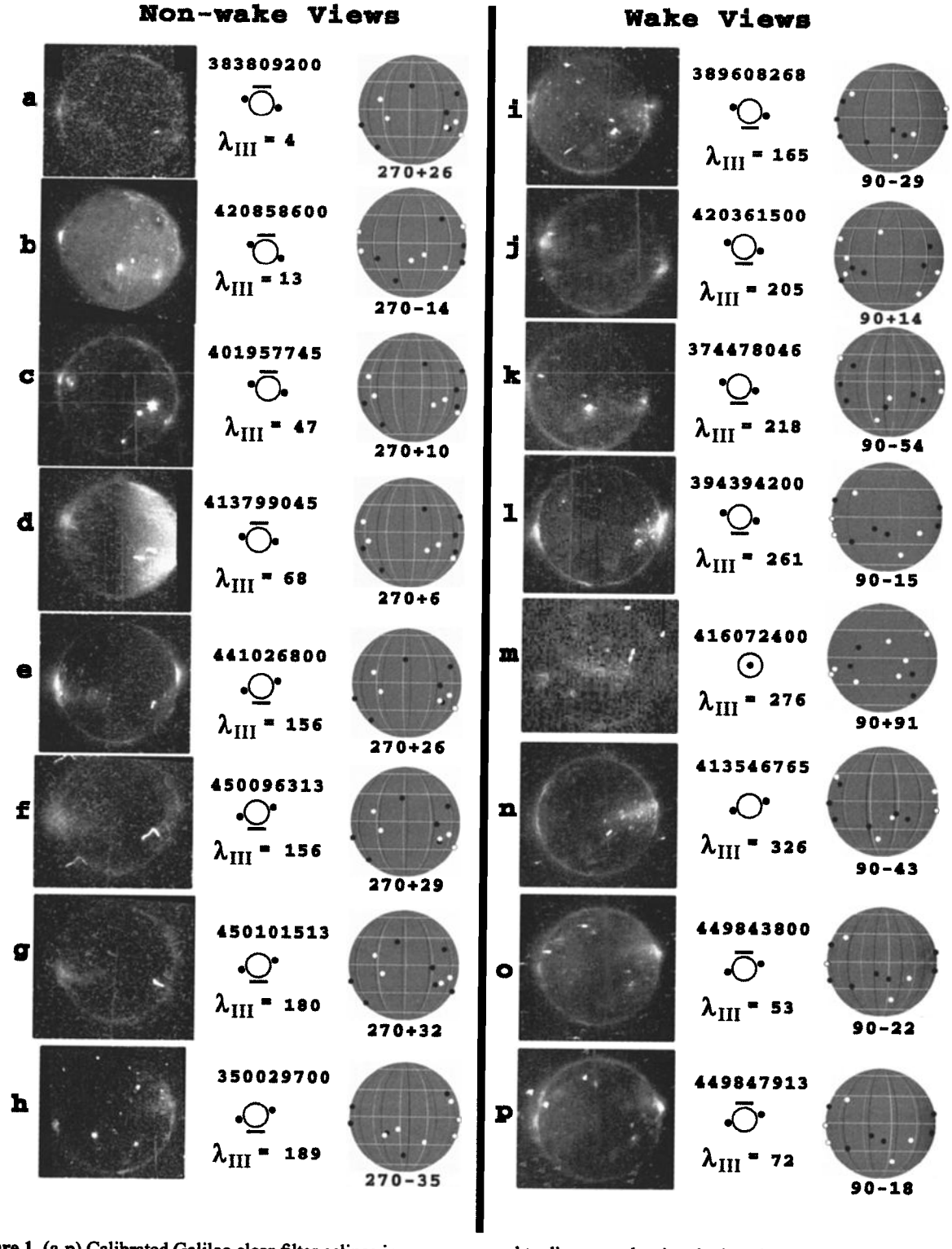

Figure 1. (a-p) Calibrated Galileo clear-filter eclipse images compared to diagrams charting the locations of volcanic vents known to be active during the Galileo Mission [*McEwen et al.* 1998a, Table VI]. Vents located on the side of Io viewed in each image are shown as white dots, while those on the opposite side of Io are shown in black (only those black dots near the limb contributed to the emissions visible in each image).

of Figure 1. The first is that the brightest equatorial emissions tend to be located where actively erupting volcanic vents occur near Io's limb. The second is that subdued emissions can be seen along the equatorial limb even in cases where no plumes are known to be active, such as at the left edge of Figure 1a.

To quantify the emission brightness, these data were first calibrated to units of W cm^{-2} sr^{-1} nm^{-1} using procedures defined by *Klaasen et al.* [1997]. These units are used because they do not require an assumption be made about the wavelength of the emissions; to convert to Rayleighs, divide by the number of joules per

Table 2. Measured Brightnesses[a]

Image Number	Plate 1 Letter	Disk Average Brightness, 10^{-13} W cm^{-2} sr^{-1} nm^{-1}	Error	Maximum Brightness Sub-Jove, 10^{-13} W cm^{-2} sr^{-1} nm^{-1}	Error	Maximum Brightness Anti-Jove, 10^{-13} W cm^{-2} sr^{-1} nm^{-1}	Error
350029700	h	4.8	3	77	9	82	15
374478046	k	21.9	5	88	12	80	12
383809200	a	14.6	6	80	4	60	8
389608268	i	24.3	3	88	9	94	4
394394200	l	22.0	2	172	11	142	19
401957745	c	12.4	1	101	13	81	17
413546765	n	22.9	5	110	15	70	5
413799045[b]	d	18.8	2	114	6	NV	NV
416072400	m	12.3	7	NV	NV	72	10
420361500	j	18.0	2	114	13	133	7
420858600	b	C	C	135	10	65	15
441026800	e	17.7	3	153	6	144	5
449843800	o	27.9	5	137	7	72	4
449847913	p	21.4	7	173	8	106	15
450096313	f	21.1	6	89	11	56	4
450101513	g	14.1	6	78	4	47	5

[a] NV, not visible in image; C, contaminated by moonlight (used for plume brightnesses only).

[b] Only left half of image used for brightness and background measurements.

photon and multiply by 4 π 10^{-6} times the bandwidth (nominally 660 nm for the clear filter). The images were spatially filtered to remove charged-particle-induced noise spikes and then hand-edited to remove larger hot spots due to thermal emission from discrete surface volcanic centers (Plate 1 and Figure 1 include both the noise spikes and the hot spots). Next, a background component was calculated for each image by computing the mean brightness of the space surrounding Io, omitting regions within half an Io radius of the disk (the emissions extend up to 700 km from the surface). Systematic variations in the background were judged to be the dominant source of error in these estimates. To determine the variability of the background we examined the corners of each image (farthest from the disk and least affected by any potential extended emission). The mean of these individual measurements differed little from the backgrounds estimated by considering all of the pixels, suggesting that any extended emission is below the detection threshold. The standard deviation of the mean of the individual measurements was taken as the formal uncertainty reported in Table 2. The background was subtracted from the measured average brightness of the disk including the limb, disk, and equatorial glows out to a height of ~700 km. The discrete volcanic centers edited earlier were left null and not counted in the disk averages. We also measured the maximum brightness of the equatorial glows at the sub-Jupiter and anti-Jupiter points, by taking the average of small areas around the brightest parts of the glows. The box size chosen was 1/20 the diameter of the disk, or 0.3% of the disk area. This is significantly smaller than the areas measured by *Retherford et al.* [2000] for equatorial spots in OI 135.6 nm images and probably contributes to the differences in the results. The intrinsic spatial heterogeneity of the equatorial spots is much larger than other sources of uncertainty in these estimates, so the errors listed in Table 2 represent the variability between measurements at several locations within the equatorial spots.

2.2 Disk Averages

Figure 2 shows the disk-averaged measurements, plotted as a function of time elapsed since Io entered eclipse. The disk-averaged brightness varies by a factor of at least 2. We have separately shown the wake views as solid circles and the nonwake views as open circles. The image labeled "m" is a very low resolution view of the anti-Jove hemisphere (neither leading nor trailing; see Plate 1m) and is represented by a half-filled circle. Only the uncontaminated half of image d is shown. In general, the wake views appear brighter than the views of the orbital trailing hemisphere. Contrary to expectations from *Geissler et al.* [1999], no discernible trend towards dimming with time elapsed in eclipse is seen. Two of the outliers (images o and f) are brighter than average, but both of these were recorded within 15 minutes of eclipse ingress. We suspect that these are contaminated by Jupiter shine on the basis of recent Cassini images that record "movies" of entire eclipses of Io [*Geissler et al.*, 2001] (see also http://ciclops.lpl.arizona.edu). These movies show brightening of the Jupiter-facing side of Io up to 15 minutes prior to eclipse egress, presumably caused by light scattered by aerosols in Jupiter's upper atmosphere. One of these images (image o) was among the pair of pictures analyzed by *Geissler et al.* [1999] and interpreted to show eclipse dimming. Two other images are anomalously dim: image j is below the average of the wake-side measurements, while image h records the faintest emissions of all. Image h is problematic in that this image was underexposed in comparison to the other pictures (Table 1), rendering faint emissions undetectable.

A possible cause of the apparently dim emissions is suggested by Figure 3, a plot of the disk averages versus magnetic longitude.

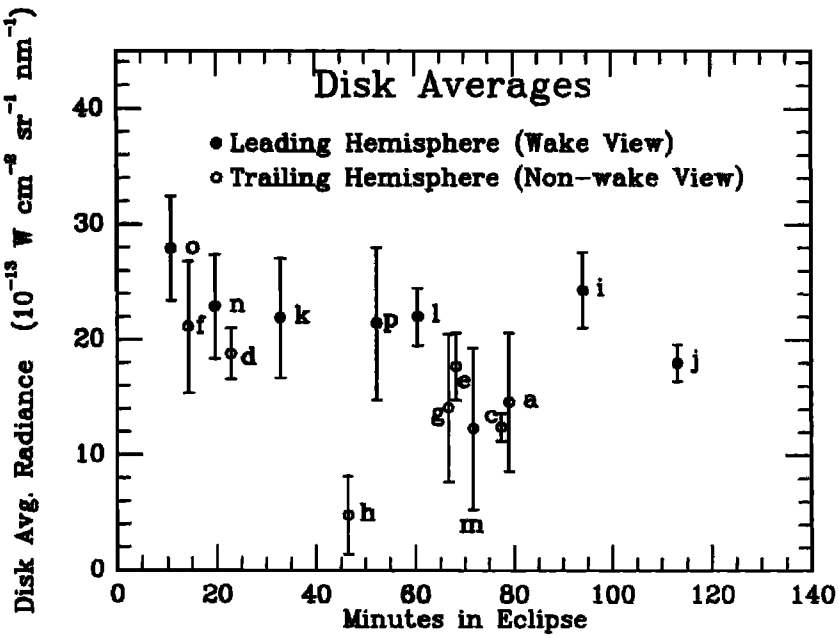

Figure 2. Disk-averaged measurements of Io's emission brightness, plotted as a function of time elapsed since Io entered eclipse. Black dots (solid circles) show the wake views (centered on the orbital leading hemisphere), and white dots (open circles) show the nonwake views (trailing hemisphere). Lowercase letters refer to individual images shown in Plate 1. Image 420858600 (Plate 1b) was omitted from the plot because of contamination by reflected light from Europa, and only the uncontaminated portion of image 413799045 (Plate 1d) was measured.

Io was farthest from the plasma torus center when image j was recorded at λ_{III} of 205°. Image h was recorded at λ_{III} of 189°, also far from the plane of the plasma torus. Several images recorded near the opposite magnetic longitude are consistent with possible dimming around 20° λ_{III}. Among the Galileo images only the distant and noisy view of the anti-Jove hemisphere in Plate 1m was recorded during plane crossing, when particle densities are expected to be greatest. No unusual brightening was detected in Plate 1m. Given the great variability of the visible emissions noted in ground-based and HST observations, however, it is likely that

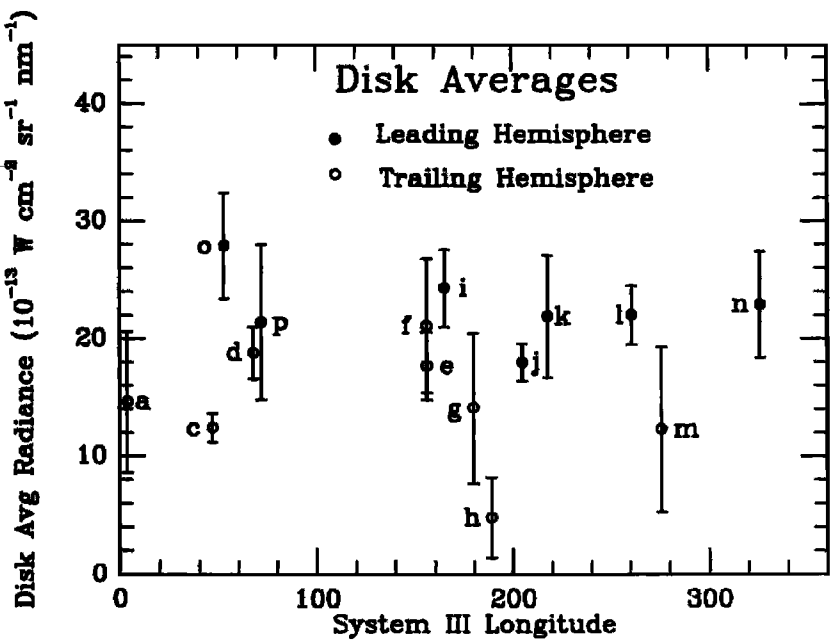

Figure 3. Disk-averaged brightness as a function of Io's Jovian magnetic longitude (λ_{III}). Lowercase letters refer to individual images shown in Plate 1.

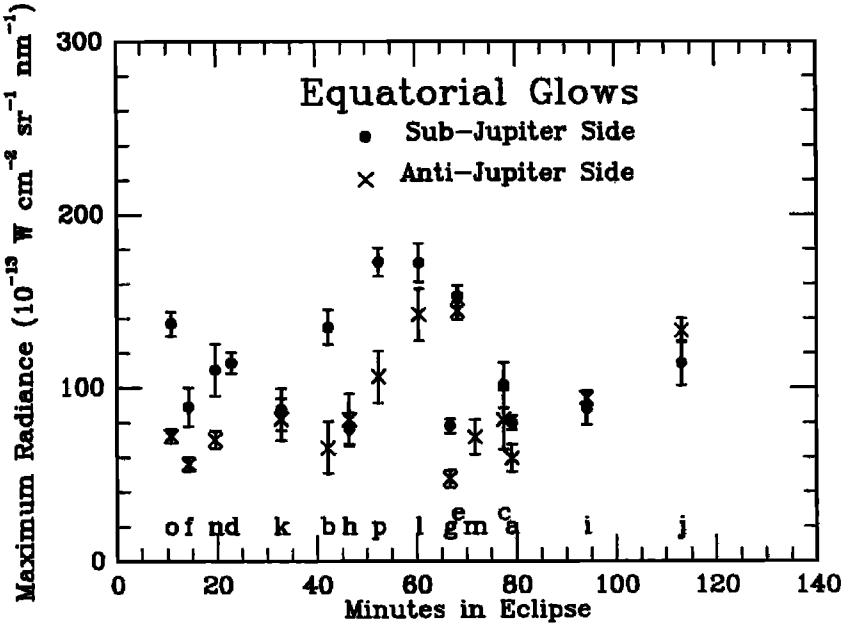

Figure 4. Maximum brightness of the equatorial glows plotted as a function of time elapsed since Io entered eclipse. Depending upon viewing geometry, at times only one or the other of these glows can be seen in the images. The plume glows on the side of Io nearest Jupiter (solid circles) are generally brighter than the glows on the opposite side (crosses). Lower case letters refer to individual images shown in Plate 1.

the Galileo data set is too small to discern any definite correlations between disk-averaged emission brightness and Jovian magnetic longitude.

2.3 Equatorial Glows

Figure 4 shows the maximum brightness of the equatorial glows plotted as a function of time elapsed since Io entered eclipse. Depending upon viewing geometry, at times only one or the other of these equatorial glows can be seen in the images. No obvious temporal trends are apparent in these data, contrary to the brightening observed during orbit 15 (images o and p). Neither are there obvious correlations with magnetic longitude, as shown by Figure 5. Unlike the disk-averages, the maximum brightness depends on the degree to which the images were smeared by camera motion while the shutter was open. However, the relative

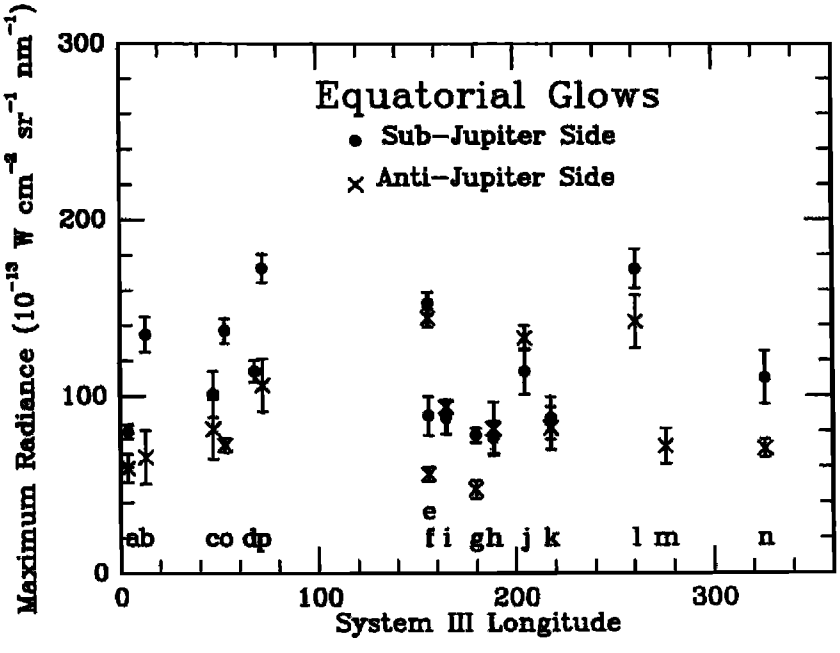

Figure 5. Maximum equatorial glow brightness as a function of Io's Jovian magnetic longitude (λ_{III}). Lowercase letters refer to individual images shown in Plate 1.

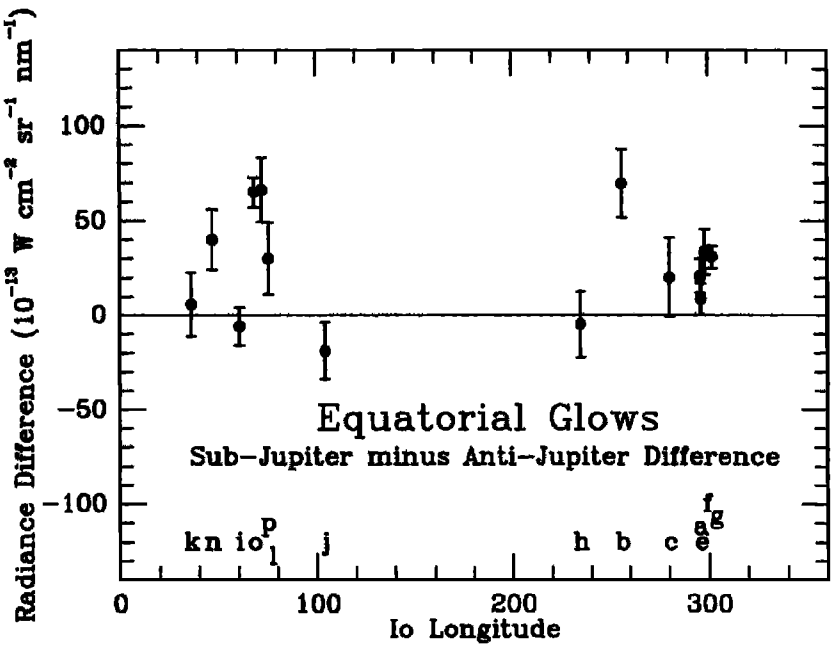

Figure 6. Equatorial glow brightness difference plotted as a function of Galileo's iocentric longitude. Positive values indicate that the maximum brightness of the equatorial glow on the inner, Jupiter-facing hemisphere was greater than that on the outer hemisphere glow.

brightness can be accurately measured and in general the brightest parts of the equatorial glows on the side of Io nearest Jupiter (solid circles) tend to be brighter than those on the opposite side (crosses). It should be understood that this brightness asymmetry relates to the brightest subspots seen in the Galileo images, regions only 90 km across. The magnitude of the brightness difference is strongly dependent on the size of the area measured, and in two cases (images k and p) the differences change sign so that the outer glow intensity exceeds the inner glow intensity when the area measured is comparable to that used by *Retherford et al.* [2000] to measure UV glow intensities (~350 km across). Although it is brighter, the equatorial glow on the Jupiter-facing hemisphere often appears to be less extensive than that on the opposite side of Io. On orbit 15 the total power radiated from the dim outer hemisphere glow was larger than that from the brighter glow on the Jupiter-facing side [*Geissler et al.*, 1999]. There is also an observational bias that favors the sub-Jupiter side of Io in 12 of the 16 images. Figure 6 shows the equatorial glow brightness differences plotted against iocentric longitude (subspacecraft longitude on Io) for all images in which both glows can be seen. Few images were centered in the longitude range from 90° to 270°, and these few include image j, an obvious exception where the Jupiter-facing equatorial plume is partially hidden from view by the limb of Io. Several pictures (images o, p, l, b, and c) that were recorded near iocentric longitudes 90° and 270° still show that the Jupiter-facing glow is brighter than the outer glow, however, and the asymmetry is apparent even in one case (image b) where the anti-Jupiter point is better seen than the sub-Jupiter side.

2.4 Polar Limb Glows

The qualitative impression from Plate 1 that the polar limb glow follows the centrifugal equator of the plasma torus is confirmed by Figure 7, a plot of the brightness difference between equal areas measured along the north and south polar limbs. The error bars shown in Figure 7 are the geometric means of the errors in the individual measurements, based upon repeatability. Figure 7 shows that, in general, the north polar limb tends to be brighter than the south over magnetic longitudes from 290° to 110° (except image n) and dimmer than the south over λ_{III} from 110° to 290°. No viewpoint bias complicates these results, because Galileo's subspacecraft latitude remained within 3° of Io's equator throughout the observations (Table 1).

3. Discussion

The visible aurorae produced by Io's atmosphere might be expected to differ substantially from its ultraviolet emissions. Visible glows can be excited by electrons with lower energies (<5 eV) than UV emissions. Near actively venting volcanoes the visible glows may be dominated by molecular emissions from SO_2. Nevertheless, several similarities between Io's visible emissions and their ultraviolet counterparts are evident. Systematic changes in the locations of the equatorial glows and the polar limb glow with λ_{III} are consistent with HST STIS observations of neutral oxygen [*Roesler et al.*, 1999; *Retherford et al.*, 2000]. The motion of Io's visible and near-ultraviolet equatorial emissions was recently recorded in one of the Cassini "movies" acquired as Io crossed the equator of the Jovian magnetic field [*Geissler et al.*, 2001]. The equatorial glows can be seen to shift in latitude, tracking the tangent points of the Jovian magnetic field lines. The enhanced emission on the wake side of Io noted in the Galileo images agrees with neutral O and S observations at ultraviolet wavelengths [*Ballester et al.*, 1997; *Wolven et al.*, 1999, this issue]. These similarities in morphology and time variability suggest that the visible and ultraviolet emissions are excited by related populations of electrons. Field-aligned Birkeland currents [e.g., *Goldreich and Lynden-Bell*, 1969] probably power the equatorial emissions, accounting for the motion of the equatorial glows with magnetic longitude. On the other hand, the polar limb glows appear to be generated by plasma torus electrons because they track the centrifugal equator of the torus. Although perhaps supplied by several sources, the electrons that stimulate the visible aurorae appear to

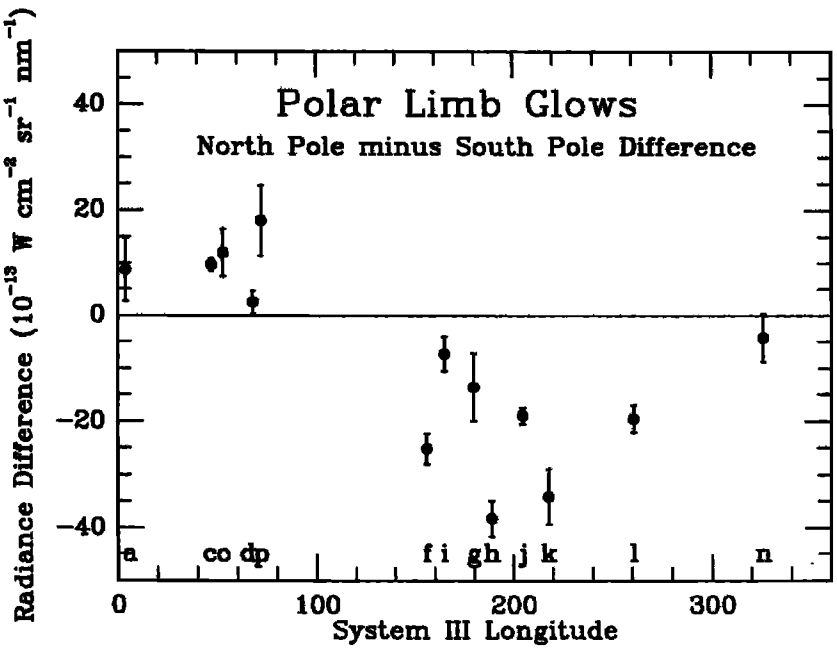

Figure 7. Polar limb glow brightness difference plotted as a function of Io's Jovian magnetic longitude (λ_{III}). Positive values indicate that the north polar glow was brighter than that along the south polar limb.

belong to the same population of electrons that stimulate the ultraviolet emissions.

A likely explanation for the leading/trailing brightness asymmetry is the enhanced plasma electron density in the wake of Io. Direct observations of the wake region by Galileo instruments suggest electron densities of up to 40,000 cm^{-3}, more than an order of magnitude greater than the background torus electron density [*Gurnett et al.*, 1996; *Frank et al.*, 1996; *Hinson et al.*, 1998]. This electron density enhancement matches the predictions of theoretical models of the flow of plasma around Io [e.g., *Linker et al.*, 1998; *Combi et al.*, 1998; *Saur et al.*, 1999].

The differences between the visible and far ultraviolet emissions appear to be due to local concentrations of SO_2 gas derived from actively venting volcanoes. Although they might be present even in the absence of volcanic activity, the equatorial glows at visible and near-ultraviolet wavelengths are greatly enhanced in the neighborhood of volcanic plumes. Near the sub-Jupiter point, enhanced emissions with characteristic plume shapes are seen near the volcano Acala in images b, c, d, i, l, o, and p. Acala's plume has not been seen in sunlight and is therefore of interest as a possible example of a relatively dust free "stealth plume," as posited by *Johnson et al.* [1995]. Concentrations of SO_2 gas at this vent may explain the greater brightness observed for the inner equatorial glow of Io than the outer hemisphere glow, in apparent contradiction of the ultraviolet results. Local brightness concentrations are seen at several other volcanoes as well, such as Prometheus (2°S, 153°W) in images l, m, o, and p; Zamama (18°N, 173°W) in images e, o, and p; Kanehekili (17°S, 36°W) in image j and perhaps Ra (8°S, 325°W) in image h. All of these volcanic centers were active during the Galileo nominal and extended missions [*McEwen et al.*, 1998a; *Keszthelyi et al.*, 2001].

Much remains unknown about Io's visible aurorae. The short-term variability of the emissions has not yet been determined; it is possible that the volcanic plumes "flicker," lighting up periodically when they are intersected by the tangent points of the Jovian magnetic field lines. It is also unclear whether the plumes provide conduits of sufficient conductivity to carry the current into Io's interior, or whether the current flows dominantly through Io's atmosphere.

4. Conclusions

Analysis of the Galileo nominal and extended mission clear-filter images of Io in eclipse supports the following conclusions about Io's visible aurora:

1. Contrary to expectations, Io's disk-averaged emissions show no general tendency to dim with time elapsed since eclipse ingress.

2. The disk-averaged emissions tend to be brighter on the orbital leading hemisphere than on the trailing hemisphere, perhaps because of enhanced electron densities in Io's plasma wake.

3. The polar limb glow correlates with Io System III longitude, such that it is brighter along the limb of the pole closest to the equator of the Jovian magnetic field.

4. The bright equatorial glows vary in location with time, corresponding in most cases to the tangent points of Jovian magnetic field lines. Local enhancements in emission are associated with specific volcanic plumes.

5. The equatorial plume glow on sub-Jupiter side frequently appears brighter and smaller than on the side of Io facing away from Jupiter. We suggest that this might be caused by local concentrations of SO_2 gas derived from active volcanoes in the region.

6. No systematic variation of equatorial glow maxima with time in eclipse is discerned, contrary to behavior observed during orbit 15. Neither is there a clear correlation of equatorial glow brightness with Jovian magnetic longitude. Such effects could be obscured by variations in surface volcanic activity or observational effects such as image smear and variations in viewing geometry.

Acknowledgments. We thank Floyd Herbert and Gilda Ballester for valuable discussions. We appreciate careful and constructive reviews by two anonymous referees. This work was partially

supported by the NASA Galileo Mission, some of which is under JPL contract 959538 to Atmospheric and Environmental Research, Inc. (WHS).

Janet G. Luhmann thanks Melissa McGrath and Ronald J. Oliversion for their assistance in evaluating this paper.

References

Ajello, J. M., G. K. James, and I. Kanik, The complete UV spectrum of SO_2 and electron impact. II, The middle ultraviolet spectrum, *J. Geophys. Res.*, *97*, 10,501-10,512, 1992.

Ballester, G. E., H. W. Moos, P. D. Feldman, D. F. Strobel, M. E. Summers, J. Bertaux, T. E. Skinner, M. C. Festou, and J. H. Lieske, Detection of neutral oxygen and sulfur emissions near Io using IUE, *Astrophys. Journ. Lett.*, *319*, L33-L38, 1987.

Ballester, G. E., J. T. Clarke, D. Rego, M. Combi, N. Larsen, J. Ajello, D. F. Strobel, N. M. Schneider, and M. McGrath, Characteristics of Io's far-UV neutral oxygen and sulfur emissions derived from recent HST observations, *Bull. Am. Astron. Soc.*, *28*, 2321-2321, 1996.

Ballester, G. E., J. T. Clarke, M. Combi, D.F. Strobel, N. Larsen, J. Ajello, N. M. Schneider, D. Rego, and M. McGrath, Characteristics of Io's far-ultraviolet emissions derived from HST, paper presented at Magnetospheres of the Outer Planets, Boulder, Colo., March 17-21, 1997.

Belton, M.J.S., et al., Galileo's first images of Jupiter and the Galilean Satellites, *Science*, *274*, 377-385, 1996.

Bouchez, A. H., M. E. Brown, and N. M. Schneider, Eclipse spectroscopy of Io's atmosphere, *Icarus*, *148*, 316-319, 2000.

Clarke, J. T., J. Ajello, J. Luhmann, N. Schneider, and I. Kanik, Hubble Space Telescope UV spectral observations of Io passing into eclipse, *J. Geophys. Res.*, *99*, 8387-8402, 1994.

Combi, M. R., K. Kabin, T. I. Gombosi, D. L. Dezeeuw, and K. G. Powell, Io's plasma environment during the Galileo flyby: Global three-dimensional MHD modeling with adaptive mesh refinement. *J. Geophys. Res.*, *103*, 9071-9082, 1998.

Cook, A. F., E. M., Shoemaker, B. A. Smith, G. E. Danielson, T. V. Johnson, and S. P. Synnott, Volcanic origin of the eruptive plumes on Io, *Science*, *211*, 1419-1422, 1981.

Frank, L. A., W. R. Paterson, K. L. Ackerson, V. M. Vasyliunas, F. V. Coroniti, and S. J. Bolton, Plasma observations at Io with the Galileo spacecraft, *Science*, *274*, 394-395, 1996.

Geissler, P.E., A.S. McEwen, W. Ip, M.J.S. Belton, T.V. Johnson, W.H. Smyth and A.P. Ingersoll. Galileo imaging of atmospheric emissions from Io, *Science*, *285*, 870-874, 1999.

Geissler, P., A. McEwen and C. Porco, Cassini imaging of auroral emissions from the Galilean Satellites, *Eos Trans. AGU*, *28*(20), Spring Meet. Suppl., abstract P51A-03, S251, 2001.

Goldreich, P., and D. Lynden-Bell, Io: A Jovian unipolar inductor, *Astrophys. J.*, *156*, 59-78, 1969.

Gurnett, D. A., W. S. Kurth, A. Roux, S. J. Bolton, and C. F. Kennel, Galileo plasma wave observations in the Io plasma torus and near Io, *Science*, *274*, 391-392, 1996.

Hinson, D. P., A. J. Kliore, F. M. Flasar, J. D. Twicken, P. J. Schinder, and R. G. Herrera, Galileo radio occultation measurements of Io's ionosphere and plasma wake, *J. Geophys. Res.*, *103*, 29,343-29,357, 1998.

Johnson, T. V., D. L. Matson, D. L. Blaney, G. J. Veeder, and A. Davies, Stealth plumes on Io, *Geophys. Res. Lett.*, *22*, 3293, 1996.

Keszthelyi, et al., Imaging of volcanic activity on Jupiter's moon Io by Galileo during Galileo Europa mission and Galileo millenium mission, *J. Geophys. Res.*, in press, 2001.

Klaasen, K. P., et al., Inflight performance characteristics, calibration, and utilization of the Galileo SSI camera, *Opt. Eng.*, *36*, 3001-3027, 1997.

Linker, J. A., K. K. Khurana, M. G. Kivelson, and R. J. Walker, MHD simulations of Io's interaction with the plasma torus, *J. Geophys. Res.*, *103*, 19,867-19,878, 1998.

McEwen, A. S., et al., Active volcanism on Io as seen by Galileo SSI, *Icarus*, *135*, 181-219, 1998a.

McEwen, A.S., et al., High-temperature silicate volcanism on Jupiter's moon Io, *Science*, *281*, 87-90, 1998b.

Miller, K. and K. Becker, Ultraviolet and visible fluorescence produced by controlled electron impact on SO_2, *Can. J. Phys.*, *65*, 530-534, 1987.

Oliversen, R.J., et al., HST/STIS visible sodium and oxygen images of Io in eclipse (abstract), *EOS Trans. AGU*, *81*, S290, 2000.

Oliversen, R. J., F. Scherb, W. H. Smyth, M. E. Freed, R. C. Woodward, M. L. Marconi, K. D. Retherford, O. L Lupie, and J.P. Morgenthaler, Sunlit Io atmospheric [O I] 6300 A emission and the plasma torus, *J. Geophys. Res.*, this issue.

Peratt, A. L., and A. J. Dessler, Filamentation of volcanic plumes on the Jovian satellite Io, *Astrophys. Space Sci.*, *144*, 451-461, 1988.

Retherford, et al., HST-Galileo Io campaign: images of sodium and oxygen emissions in eclipse, *Eos Trans. AGU*, *80*(46), Fall Meet. Suppl., P41A-05, 1999.

Retherford, K. D., H. W. Moos, D. F. Strobel, B. C. Wolven, and F.L. Roesler, Io's equatorial spots: Morphology of the neutral UV emissions, *J. Geophys. Res.*, *105*, 27,157-27,165, 2000.

Roesler, F. L., H. W. Moos, R. J. Oliversen, R. C. Woodward, K. D. Retherford, F. Scherb, M. A. McGrath, W. H. Smyth, P. D. Feldman, and D. F. Strobel, Far-ultraviolet imaging spectroscopy of Io's atmosphere with HST/STIS, *Science*, *283*, 353-357, 1999.

Saur, J., F. M. Neubauer, D. F. Strobel, and M. E. Summers, Three-dimensional plasma simulation of Io's interaction with the Io plasma torus: Asymmetric plasma flow, *J. Geophys. Res.*, *104*, 25,105-25,126, 1999.

Saur, J., F. M. Neubauer, D. F. Strobel, and M. E. Summers, Io's ultraviolet aurora: Remote sensing of Io's interaction, *Geophys. Res. Lett.*, 27, 2893-2896, 2000.

Scherb, F., and W. Smyth, Variability of (O I) 6300-A emission near Io, *J. Geophys. Res.*, *98*, 18,729-18,736, 1993.

Scherb, F., R. J. Oliversen, M. E. Freed, J. Corliss, R. C. Woodward, W. H. Smyth, J. P. Morgenthaler, O. L. Lupie, and K. D. Retherford, Ground-Based observations of [OI] 6300 angstroms emission from Io (abstract), *Bull. Am. Astron. Soc.*, *31*, 1166, 1999.

Trauger, J. T., K. R., Stapelfeldt, G. E. Ballester, J. T. Clarke, and the WFPC2 Science Team, HST Observations of [OI] Emissions from Io in eclipse (abstract), *Bull. Am. Astron. Soc.*, *29*, 1002, 1997.

Wolven, B. C., H. W. Moos, P. D. Feldman, K. D. Retherford, D. F. Strobel, W. H. Smyth, F. L. Roesler, and R. J. Oliversen, Emission profiles of neutral oxygen and sulfur in Io's exospheric corona (abstract), *Bull. Am. Astron. Soc.*, *31*, 1166, 1999.

Wolven, B. C., H. W. Moos, K. D. Retherford, P. D. Feldman, D. F. Strobel, W. H. Smyth, and F. L. Roesler, Emission profiles of neutral oxygen and sulfur in Io's exospheric corona, *J. Geophys. Res.*, this issue.

M.J.S. Belton, Belton Space Exploration Initiatives, 430 S. Randolph Way, Tucson AZ 85716 USA (belton@azstarnet.com)

A.J. Dessler, P.E. Geissler, W. Hubbard and A. McEwen, Lunar and Planetary Laboratory, University of Arizona, Tucson, AZ 85721, USA (dessler@arizona.edu, geissler@lpl.arizona.edu, hubbard@lpl.arizona.edu, mcewen@jupiter.lpl.arizona.edu)

A.P. Ingersoll, Division of Geology and Planetary Sciences, California Institute of Technology, Pasadena CA 91125 USA. (api@helene.gps.caltech.edu)

W. Ip, Institute of Astronomy, National Central University, Chung-Li, Taiwan 320, ROC. (wingip@joule.phy.ncu.edu.tw)

T.V. Johnson, Jet Propulsion Laboratory, MS 264-419, 4800 Oak Grove Drive, Pasadena CA 91109 USA

K. Rages, Space Physics Research Institute, Sunnyvale, CA 94085 USA (rages@darkstar.arc.nasa.gov)

W.H. Smyth, Atmospheric and Environmental Research, Inc., 840 Memorial Dr., Cambridge MA 02139 USA. (William_Smyth@aer.com)

(Received December 28, 2000; revised June 6, 2001;
accepted June 6, 2001.)